EurJIC European Journal of Inorganic Chemistry

ChemPubSoc Europe

FULL PAPER

DOI:10.1002/ejic.201501109

Intramolecular C–O Insertion of a Germanium(II) Salicyl Alcoholate: A Combined Experimental and Theoretical Study

Philipp Kitschke,[a] Tobias Rüffer,[b] Marcus Korb,[b] Heinrich Lang,[b] Wolfgang B. Schneider,[c] Alexander A. Auer,[c] and Michael Mehring*[a]

Keywords: Germanium / Germylenes / Insertion / Density functional calculations

The synthesis of germanium(II) 2-*tert*-butyl-4-methyl-6-(oxidomethyl)phenolate (**1**) starting from $Ge[N(SiMe_3)_2]_2$ and the corresponding salicyl alcohol is reported. Compound **1** undergoes an intramolecular oxidative insertion reaction of germanium into a C–O bond to result in a cyclic germanium(IV) tetraoxidogermocane (**2**). Addition of 3-*tert*-butyl-2-hydroxy-5-methylbenzyl alcohol to either compound **1** or **2** gave a spirocyclic monoorgano dioxagermine (**3**). The results of ^1H NMR spectroscopic studies and DFT-D calculations are in agreement with the proposed reaction cascade in which the novel germylene **1** is first converted into the germocane **2** followed by reaction with 3-*tert*-butyl-2-hydroxy-5-methylbenzyl alcohol to finally provide compound **3**. Addition of 4-(dimethylamino)pyridine to a solution of germylene **1** resulted in the formation of an air-stable monomeric 1:1 complex (**4**). The characterization of compounds **1**–**4** by single-crystal X-ray diffraction analysis, thermal analysis, and ^1H NMR, $^{13}C\{^1H\}$ NMR, and ATR-FTIR spectroscopy is presented.

Introduction

Since Harris and Lappert reported on the synthesis of $Ge[N(SiMe_3)_2]_2$ in 1974[1] an ongoing and increasing interest in low-valent germanium(II) molecules has been observed, mainly attributed to their analogous carbene character. Recent studies on germylenes have focused on their use as ligands in transition-metal complexes,[2] their potential in catalysis,[3] and their application as model compounds in mechanistic studies of oxidative addition reactions.[2d,4] The majority of these studies follow the concept of Harris and Lappert, which is based on applying amide ligands, usually possessing bulky substituents, to stabilize the low-valent metal.[2e,5] Studies on germylenes based on alkoxides have been less frequently reported in the literature. The use of a sterically demanding backbone in the alkoxide/aryloxide ligand, mainly based on phenolates, has been a prerequisite to obtaining stable compounds.[6] Alkoxide-based germylenes possessing less bulky ligands have to be stabilized by additional intramolecular coordination, for example, by using amines, as reported by Huang and co-workers as well as recently by Heidemann and Mathur.[7] Following the concept of intermolecular donor stabilization, Wetherby et al. were able to synthesize the cyclic germanium(II) aryloxide (*S*)-[Ge{$O_2C_{20}H_{10}(SiMe_2Ph)_2$-3,3′}{$NH_3$}].[8] In addition, cyclic germanium(II) aryloxides possessing additional intramolecular coordination of oxygen atoms have been reported for calixarene derivatives.[9]

Germylenes lacking additional stabilization are known to undergo oxidative insertion reactions according to their electron deficiency at the germanium atom. Thus, insertion into a diverse range of bond types, such as H–X (X = H,[10] CH_2R,[11] CN,[4d] NH_2,[10] N_3,[4d] and PH_2[4c]), C–Y (Y = Cl,[12] Br,[13] and I[7b,13,14]), N–Br,[15] P–Cl,[16] and E–E (E = S[7b,14a,14c] and O[14c]), as well as the oxidative addition of Br_2[7b,14a] have been reported. Noteworthy, to the best of our knowledge, the insertion into a C–H bond mediated by a Lewis acid to give a germaindane starting from bis(2,4,6-tri-*tert*-butylphenyl)germylene is the only reported example of an intramolecular insertion reaction for germylenes.[11c,17]

Herein we report on the synthesis and reactivity of germanium(II) 2-*tert*-butyl-4-methyl-6-(oxidomethyl)phenolate (**1**), which is the first example of an unsymmetrical cyclic

[a] Technische Universität Chemnitz, Fakultät für Naturwissenschaften, Institut für Chemie, Professur Koordinationschemie,
Straße der Nationen 62, 09111 Chemnitz, Germany
E-mail: michael.mehring@chemie.tu-chemnitz.de
www.tu-chemnitz.de/chemie/koord/
[b] Technische Universität Chemnitz, Fakultät für Naturwissenschaften, Institut für Chemie, Professur Anorganische Chemie,
Straße der Nationen 62, 09111 Chemnitz, Germany
[c] Max-Planck-Institut für Chemische Energiekonversion, Stiftsstraße 34–36, 45470 Mülheim an der Ruhr, Germany
Supporting information for this article is available on the WWW under http://dx.doi.org/10.1002/ejic.201501109.

germanium(II) compound exhibiting both an aryloxide and an alkoxide moiety (Scheme 1). The dynamic coordination behavior and the reactivity of compound **1** in the presence as well as in the absence of 3-*tert*-butyl-2-hydroxy-5-methylbenzyl alcohol and 4-(dimethylamino)pyridine were studied, revealing an intramolecular oxidation reaction that leads to a cyclic tetraoxidogermocane (**2**), a spirocyclic dioxagermine (**3**), and a 4-(dimethylamino)pyridine complex (**4**; Scheme 1). ^{1}H NMR spectroscopic studies and DFT-D calculations (B3LYP-D3/def2-TZVPP level of theory) were carried out to identify the reaction paths that compounds **1** and **2** follow to form the monoorgano germanium(IV) alcoholate **3**.

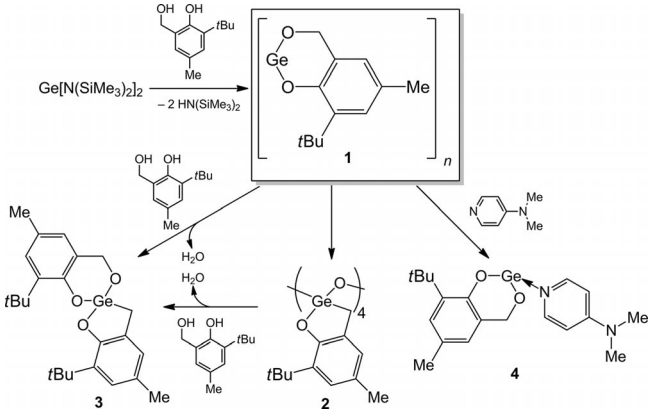

Scheme 1. Synthesis of compounds **1**–**4**. Germylene **1** forms a trimer (n = 3) in the solid state, whereas an equilibrium (n = 2, 3, 4) is observed in solution.

Results and Discussion

Syntheses and Characterization

Compound **1** was synthesized starting from $Ge[N(SiMe_3)_2]_2$ and 3-*tert*-butyl-2-hydroxy-5-methylbenzyl alcohol in *n*-pentane and isolated as a colorless solid in 83% yield (Scheme 1).

Compound **1** is soluble in all common polar and nonpolar organic solvents. Crystallization from a saturated diethyl ether solution gave crystals within 1 hour suitable for single-crystal X-ray diffraction analysis. ^{1}H and ^{1}H–^{13}C{^{1}H} HSQC NMR spectroscopic analyses of a freshly prepared solution of either crystalline or amorphous **1** in $CDCl_3$ at ambient temperature gave resonance signals (three sets of signals assigned to the *t*Bu, Me, and CH_2 groups, respectively, and six signals assigned to aromatic CH groups) that are in agreement with the trimeric structure observed in the solid state (Figure 1). One set of additional resonance signals of lower intensity possessing similar chemical shifts and integral ratios was also observed, which indicates the presence of at least one additional oligomer of germylene **1** (see Figure S1 in the Supporting Information). Cooling the $CDCl_3$ solution of **1** to –60 °C resulted in two independent sets of additional resonance signals of lower intensity, which were assigned to symmetrical oligomers of **1** (e.g., n = 2, 4) according to the quantity and multiplicity of these signals (see Figure S2). The single-crystal X-ray diffraction analysis revealed the formation of a trimer of germylene **1** in the solid state [2(**1**)$_3$·Et$_2$O] that crystallizes in the monoclinic space group $P2_1/c$. The molecular structure is given in Figure 1 and selected bond lengths and angles are presented in the caption. Details of the structure determination are summarized in Table 2.

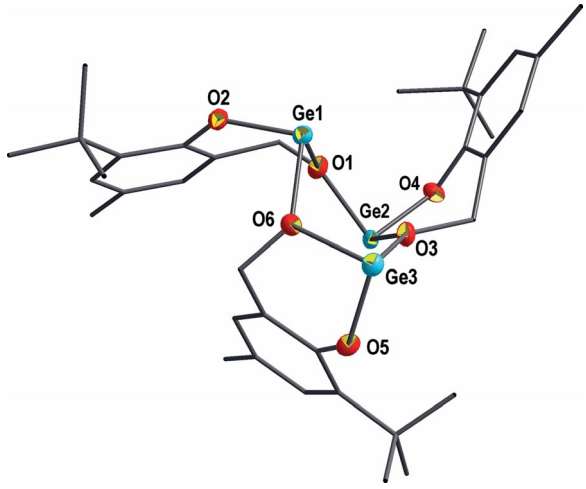

Figure 1. Molecular structure of (**1**)$_3$ in the solid state. Thermal ellipsoids are drawn at the 50% probability level. Hydrogen atoms have been omitted and aromatic moieties are depicted in wireframe style for clarity. Selected bond lengths [Å]: Ge1–O1 1.945(2), Ge1–O2 1.862(2), Ge1–O6 2.003(2), Ge2–O1 2.044(2), Ge2–O3 2.019(2), Ge2–O4 1.890(2), Ge3–O3 2.015(2), Ge3–O5 1.829(3), Ge3–O6 1.956(2); selected bond angles [°]: Ge1–O1–Ge2 127.73(11), Ge3–O3–Ge2 132.29(11), Ge3–O6–Ge1 112.79(11), O2–Ge1–O1 91.88(9), O2–Ge1–O6 97.24(9), O1–Ge1–O6 90.65(9), O4–Ge2–O3 91.32(9), O4–Ge2–O1 96.00(9), O3–Ge2–O1 83.22(9), O5–Ge3–O6 92.69(9), O5–Ge3–O3 95.95(9), O6–Ge3–O3 85.21(9).

The trimer (**1**)$_3$ shows a distorted boat conformation of the six-membered –[Ge1–O1–Ge2–O3–Ge3–O6]– ring. The germanium atoms are tricoordinated by one terminal phenolic oxygen atom and two bridging benzylic oxygen atoms. The germanium oxygen bond lengths [O_{Aryl}–Ge bonds: 1.829(2)–1.890(2) Å, O_{Alkyl}–Ge bonds: 1.945(2)–2.044(2) Å] are in the typical ranges reported for these types of bonds in compounds with a three-fold pyramidal coordination of low-valent germanium.[6b,6c,9a] The Ge1–O1 [1.945(2) Å], Ge2–O3 [2.019(2) Å], and Ge3–O6 [1.956(2) Å] bond lengths are shorter than the Ge1–O6 [2.003(2) Å], Ge2–O1 [2.044(2) Å], and Ge3–O3 [2.015(2) Å] bond lengths, respectively, which indicates that the secondary bonding of O1→Ge2, O3→Ge3, and O6→Ge1 stabilize the low-valent species. The small O–Ge–O bond angles of the salicylic moieties [O2–Ge1–O1 91.88(9)°, O4–Ge2–O3 91.32(9)°, and O5–Ge3–O6 92.69(9)°] as well as the angles [∠O1–O3–Ge2–O4 89.146(2)°, ∠O3–O5–Ge3–O6 90.580(2)°, and ∠O6–O2–Ge1–O1 95.567(2)°] between the additionally coordinating benzylic oxygen atoms (O1→Ge2, O3→Ge3, and O6→Ge1) and the planes spanned by the germanium atoms and the oxygen atoms of the salicylic moiety (O3–Ge2–O4, O5–Ge3–O6, and O2–Ge1–O1) are in agreement with low-

valent germanium possessing a stereochemically active lone pair of electrons. The bridging benzylic oxygen atoms donate electron density into the vacant p orbitals. The larger deviation of the angle ∠O6–O2–Ge1–O1 [95.567(2)°] from the ideal value of 90° might result from repulsion effects of the sterically demanding salicylic moieties that are in close proximity to each other.

Attempts to crystallize compound **1** from a 1,4-dioxane solution at ambient temperature gave [**2**·$(C_4H_8O_2)_2$]·$3C_4H_8O_2$ in an overall yield of 80% after 2 weeks. Similarly, compound **2** was also isolated starting from a solution of germylene **1** in diethyl ether in 67% yield after 5 days (Scheme 1). ^{1}H NMR spectroscopic analysis of **2**, which is soluble in common organic solvents, gave multiple resonance signals at chemical shifts centered at δ = 1.4, 2.2, 2.5, and 6.9 ppm with integral ratios of 9:3:2:2 assigned to the *t*Bu, Me, CH_2, and CH groups, respectively. The carbon atoms of the methylene groups are located at δ = 15.3 ppm, as determined by ^{1}H–^{13}C{^{1}H} HSQC and ^{13}C{^{1}H} NMR spectroscopy. Analysis of the thermal behavior of the powder obtained from crystalline [**2**·$(C_4H_8O_2)_2$]·$3C_4H_8O_2$ on drying under an inert atmosphere (see Figures S3 and S4 in the Supporting Information) revealed that two molecules of 1,4-dioxane are released at 98 °C followed by melting with an onset temperature of 159 °C and decomposition at 260 °C by endothermic processes. Compound [**2**·$(C_4H_8O_2)_2$]·$3C_4H_8O_2$ crystallizes in the triclinic space group $P\bar{1}$. Its molecular structure is given in Figure 2 and selected bond lengths and angles are presented in the caption. Details of the structure determination are summarized in Table 2.

Compound **2** is monomeric in the solid state, possessing a corrugated eight-membered –[Ge1–O2–Ge2–O4–Ge1′–O2′–Ge2′′–O4′′]– ring. Germasesquioxanes and cyclic diorgano germanium oxides have been reported to exhibit similar structural motifs of eight-membered –[Ge–O]$_4$– cycles.[18] The molecular structure of [**2**·$(C_4H_8O_2)_2$] exhibits C_i symmetry with the center of inversion located in the plane spanned by the four germanium atoms. The equivalent germanium atoms Ge1 and Ge1′ are pentacoordinated, showing a distorted trigonal-bipyramidal coordination sphere by bonding to two bridging oxygen atoms and a carbon atom in the equatorial positions, and a phenolic oxygen atom and an additional oxygen atom from 1,4-dioxane in the axial positions, respectively. The second set of equivalent germanium atoms (Ge2 and Ge2′′) are surrounded by two bridging oxygen atoms, an oxygen, and a carbon atom of the aromatic moiety resulting in a distorted tetrahedral coordination. The germanium–oxygen bond lengths of the bridging oxygen atoms are slightly shorter for the oxygen atoms bound to Ge2 [Ge2–O2 1.730(6) Å, Ge2–O4 1.744(6) Å] than for those bound to Ge1 [Ge1–O2 1.755(6) Å, Ge1–O4′′ 1.761(5) Å]. The latter holds for the germanium–oxygen bonds connected to the aromatic moiety [Ge1–O1 1.832(6) Å compared with Ge2–O3 1.805(6) Å], whereas the germanium–carbon bonds Ge1–C7 and Ge2–C19 were determined to have bond lengths of 1.913(8) and 1.921(8) Å, respectively. However, all the bond lengths are in agreement with those found in germanium(IV) compounds, such as

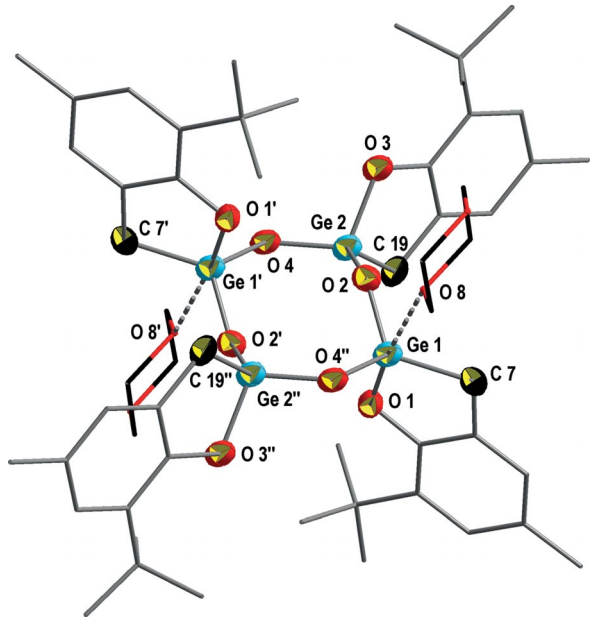

Figure 2. Molecular structure of [2·$(C_4H_8O_2)_2$] in the solid state. Thermal ellipsoids are drawn at the 50% probability level. Hydrogen atoms have been omitted for clarity. The two weakly coordinated solvent molecules and the aromatic moieties are depicted in wireframe style for clarity. Selected bond lengths [Å]: Ge1–O1 1.832(6), Ge1–O2 1.755(6), Ge1–O4′′ 1.761(5), Ge1–O8 2.447(6), Ge1–C7 1.913(8), Ge2–O2 1.730(6), Ge2–O3 1.805(6), Ge2–O4 1.744(6), Ge2–C19 1.921(8); selected bond angles [°]: O1–Ge1–O2 102.9(3), O1–Ge1–O4′′ 103.4(3), O1–Ge1–C7 92.9(3), O2–Ge1–O4′′ 109.2(3), O2–Ge1–C7 122.2(3), O4′′–Ge1–C7 120.5(3), O1–Ge1–O5 173.4(2), O2–Ge2–O3 103.3(3), O2–Ge2–O4 110.0(3), O2–Ge2–C19 120.2(3), O3–Ge2–O4 107.3(3), O3–Ge2–C19 95.0(3), O4–Ge2–C19 117.9(3), Ge1–O2–Ge2 133.4(3). Symmetry transformation used to generate equivalent atoms: ′ –*x* + 2, –*y*, –*z* + 1; ′′ –*x* + 2, –*y* + 2, –*z*.

$(Ph_2GeO)_4$,[18a] $(tBu_2GeO)_3$,[19] $2tBu_2Ge(OH)_2$·$(tBu_2GeOH)_2O$·H_2O,[20] $[Ge(L^1)_2]_2$ (L^1 = *cis*-1,2-cyclopentanediolate), and $Ge(OCH_3)(L^2)(L^3)$[21] (L^2 = *cis*-oxolane-3,4-diolate, L^3 = *cis*-oxolane-3-ol-4-olate). Note that the distances between the oxygen atoms of the coordinating 1,4-dioxane molecules and the germanium atoms [Ge1–O5 2.447(6) Å] are significantly shorter than the sum of their van der Waals radii (3.63 Å),[22] and thus heat treatment at temperatures above 98 °C is necessary to remove the coordinated molecules.

The formation of compound **3** starting from germylene **1** was detected by NMR spectroscopic monitoring of a solution of **1** in $CDCl_3$ over several days without rigorous exclusion of moisture. The dioxagermine **3** results from an intramolecular oxidative insertion reaction of the germylene **1** and subsequent reaction with 3-*tert*-butyl-2-hydroxy-5-methylbenzyl alcohol. The formation of 3-*tert*-butyl-2-hydroxy-5-methylbenzyl alcohol results from the partial hydrolysis of **1** due to the presence of traces of moisture. Pristine **3** was obtained as colorless needles after stirring compound **1** under reflux for 21 h in 1,4-dioxane, work-up, and crystallization from 1,4-dioxane/CH_2Cl_2. The equimolar addition of 3-*tert*-butyl-2-hydroxy-5-methylbenzyl alcohol to a solution of germylene **1** in diethyl ether stored

over molecular sieves gave compound **3** in 70% yield. Similarly, the reaction of germocane **2** with 4 equiv. of 3-*tert*-butyl-2-hydroxy-5-methylbenzyl alcohol in diethyl ether stored over molecular sieves provided the spirocyclic compound **3** in 41% yield (Scheme 1). Two sets of characteristic AB resonance signals for the diastereotopic methylene protons of compound **3** at δ = 2.59–2.64 and 5.04–5.12 ppm assigned to CH_2Ge and CH_2O, respectively, are present in its ^1H NMR spectrum. The respective methylene carbon atoms resonate at chemical shifts of δ = 13.1 (CH_2Ge) and 67.2 ppm (CH_2O), as determined by ^1H–$^{13}C\{^1H\}$ HSQC and $^{13}C\{^1H\}$ NMR spectroscopy. Note that compound **3** exhibits an equilibrium between its monomer and dimer $(\mathbf{3})_2$ in solution, as determined by temperature-dependent NMR spectroscopy (see Figure S5 in the Supporting Information). Analysis of the thermal behavior of **3** (see Figures S3 and S4) revealed an exothermic decomposition instantly after melting at 213 °C. Compound **3**, which is soluble in common organic solvents, crystallizes from 1,4-dioxane/CH_2Cl_2 as a dimer in the monoclinic space group $P2_1/n$. The molecular structure of $(\mathbf{3})_2$ is given in Figure 3 and selected bond lengths and bond angles are presented in the caption. Details of the structure determination are summarized in Table 2.

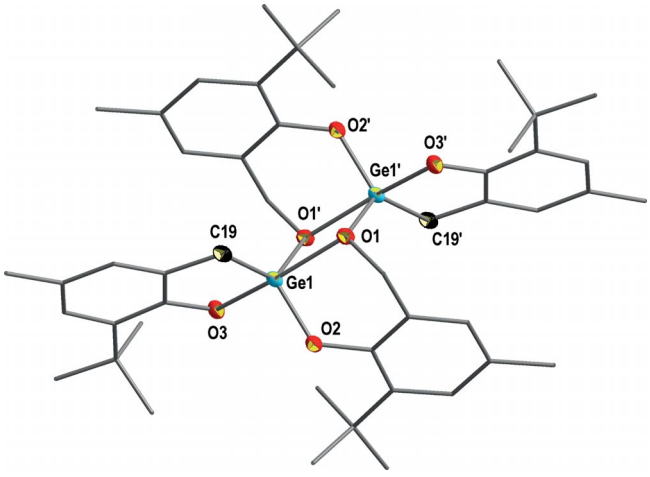

Figure 3. Molecular structure of $(\mathbf{3})_2$ in the solid state. Thermal ellipsoids are drawn at the 50% probability level. Hydrogen atoms have been omitted and aromatic moieties are depicted in wireframe style for clarity. Selected bond lengths [Å]: Ge1–O1 2.1248(15), Ge1–O2 1.7779(15), Ge1–O3 1.8324(15), Ge1–O1′ 1.8311(15), Ge1–C19 1.935(2); selected bond angles [°]: O1–Ge1–O2 88.45(6), O1–Ge1–O3 170.35(6), O1–Ge1–O1′ 74.81(7), O1–Ge1–C19 93.68(8), O2–Ge1–O3 95.09(7), O2–Ge1–O1′ 107.04(7), O2–Ge1–C19 123.25(8), O3–Ge1–O1′ 95.56(6), O3–Ge1–C19 91.87(8), C19–Ge1–O1′ 128.19(9). Symmetry transformation used to generate equivalent atoms: ′ $-x + 1, -y, -z + 1$.

The dimer $(\mathbf{3})_2$ exhibits C_i symmetry with the center of inversion located in the plane spanned by the Ge1, O1, Ge1′, and O1′ atoms. The equivalent benzylic oxygen atoms O1 and O1′ bridge the germanium atoms, which possess a distorted trigonal-bipyramidal coordination formed of four oxygen atoms and one carbon atom in an equatorial position. The Ge1–O1 [2.1248(15) Å] bond is significantly longer than the Ge1–O1′ [1.8311(15) Å] bond, which is in agreement with the respective positions of the bridging oxygen atoms (axial position with longer bond length; equatorial position with shorter bond length). The same trend is observed on comparing the bond lengths between the phenolic oxygen atoms and the germanium atom; the Ge1–O3 bond [1.8324(15) Å, axial position] is significantly longer than the Ge1–O2 bond [1.7779(15) Å, equatorial position]. A similar structural motif exhibiting an equivalent ordering of the oxygen–germanium bond lengths has been reported for $[Ge(L^1)_2]_2$ by Klüfers and Vogler.[21] All bond lengths are within typical ranges for germanium(IV) compounds possessing Ge–C and Ge–O bonds, as reported for $(t\mathrm{Bu}_2\mathrm{GeO})_3$,[19] $2t\mathrm{Bu}_2\mathrm{Ge(OH)}_2\cdot(t\mathrm{Bu}_2\mathrm{GeOH})_2\mathrm{O}\cdot\mathrm{H}_2\mathrm{O}$,[20] $[Ge(L^1)_2]_2$, and $Ge(OCH_3)(L^2)(L^3)$.[21]

As outlined above, germylene **1** is not stable in solution and hence undergoes intramolecular C–O insertion. However, we believed that it might be stabilized by the addition of donor ligands, as reported for other germylenes.[5c,23] Thus, stoichiometric amounts of 4-(dimethylamino)pyridine were added to a solution of **1** and finally compound **4**, as the corresponding 4-(dimethylamino)pyridine complex (1:1), was isolated in 75% yield (Scheme 1). Compound **4** neither decomposes in air in the solid state for at least 1 week, as determined by ATR-FTIR spectroscopy, nor does it undergo any reaction in solution (diethyl ether and/or $CDCl_3$) at ambient temperature, even in the presence of stoichiometric amounts of 3-*tert*-butyl-2-hydroxy-5-methylbenzyl alcohol. However, it decomposes in toluene solution at elevated temperatures (100 °C) to give 4-(dimethylamino)pyridine and germocane species such as **2**. The presence of moisture in $CDCl_3$ solutions of complex **4** resulted in the formation of spirocyclic germanium(IV) compound **3**. NMR spectroscopic analysis of the germylene complex **4** gave 8 and 14 resonance signals in the ^1H and $^{13}C\{^1H\}$ NMR spectra, respectively. The multiplicity pattern, in addition to the small widths of half signal height in the ^1H NMR spectrum, indicates that the complex is monomeric in solution, in accordance with its molecular structure in the solid state. Analysis of the thermal behavior (see Figures S3 and S4 in the Supporting Information) revealed an exothermic decomposition instantly after melting at 143 °C. Germanium(II) complex **4** crystallizes from diethyl ether in the monoclinic space group $P2_1/n$. Its molecular structure is given in Figure 4 and selected bond lengths and bond angles are presented in the caption. Details of the structure determination are summarized in Table 2.

Complex **4** is monomeric in the solid state, possessing pyramidal geometry at the germanium atom. The Ge1–O1 [1.8151(16) Å], Ge1–O2 [1.8765(15) Å], and Ge1–N1 [2.0990(18) Å] bond lengths are in good agreement with values reported for the germylene complex [Py(CH_2C-Ph_2O)(CH_2CMe_2O)Ge] [Ge–O(CMe_2CH_2) 1.827(1) Å, Ge–O(CPh_2CH_2) 1.881(1) Å, and Ge–N 2.110(1) Å].[7c] The recently reported 4-(dimethylamino)pyridine complex of $GeCl_2$ exhibits a similar $Ge–N_{pyridine}$ bond length of 2.028(2) Å.[23a] The Ge1–O1 bond (monodentate benzylic oxygen) is shorter than the Ge1–O2 bond (monodentate phenolic oxygen) and the corresponding bonds of the

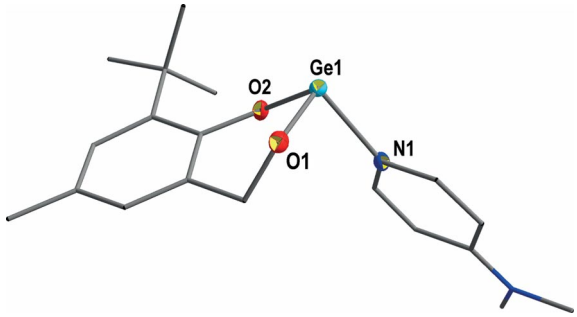

Figure 4. Molecular structure of the germylene complex **4** in the solid state. Thermal ellipsoids are drawn at the 50% probability level. Hydrogen atoms have been omitted and aromatic moieties are depicted in wireframe style for clarity. Selected bond lengths [Å]: Ge1–O1 1.8151(16), Ge1–O2 1.8765(15), Ge1–N1 2.0990(18); selected bond angles [°]: O1–Ge1–O2 96.04(7), O1–Ge1–N1 94.73(7), O2–Ge1–N1 88.75(7).

germylene $(\mathbf{1})_3$ [Ge1–O1 1.945(2) Å, Ge2–O3 2.019(2) Å, and Ge3–O6 1.956(2) Å] possessing bridging benzylic oxygen atoms. The bond angles ∠O1–Ge1–O2 [96.04(7)°], ∠O1–Ge1–N1 [94.73(7)°], and ∠O2–Ge1–N1 [88.75(7)°; Σ 279.52(21)°] are in agreement with a stereochemically active lone pair of electrons at germanium and donation of additional electron density from the pyridine nitrogen atom into the vacant p-type orbital.

In summary, the germylene **1** is trimeric in the solid state and shows dynamic coordination behavior in solution. It is quite stable in the presence of donors, but smoothly converts into the germanium(IV) species by intramolecular insertion of germanium into the benzylic C–O bonds, as exemplified by the isolation of germocane **2**. In the presence of 3-*tert*-butyl-2-hydroxy-5-methylbenzyl alcohol, which may result from partial hydrolysis, reaction to give the spirocyclic germanium(IV) compound **3** was observed. To identify the reaction paths by which **1** is converted into compounds **2** and/or **3**, ^{1}H NMR spectroscopic studies and DFT-D calculations were carried out.

^{1}H NMR Spectroscopic Studies

Four ^{1}H NMR spectroscopic experiments were carried out to study the reactions. Freshly prepared [D_8]toluene solutions of i) pure germylene **1**, ii) an equimolar mixture of **1** and 3-*tert*-butyl-2-hydroxy-5-methylbenzyl alcohol, iii) a mixture of germocane **2** and 4 equiv. of 3-*tert*-butyl-2-hydroxy-5-methylbenzyl alcohol, and iv) a solution of compound **3** in water-saturated $CDCl_3$ were monitored for at least 136 h (Scheme 2).

Experiment i) revealed a slow conversion of germylene **1** into germocane species (98%) within 190 h (see Figure S6 in the Supporting Information). The formation of minor amounts of compound **3** (2%) was also determined in experiment i) due to the high sensitivity of germylene **1** towards hydrolysis, which gives 3-*tert*-butyl-2-hydroxy-5-methylbenzyl alcohol. The latter reacts with compound **1** to give the spirocyclic compound **3** (see above). Analysis of the evolution of the resonance signals assigned to compounds **1–3** revealed that **3** is initially formed at the same time as the germocanes. However, the formation of compound **3** ceased as the conversion of germylene **1** into germocanes progressed (see Figure S6).

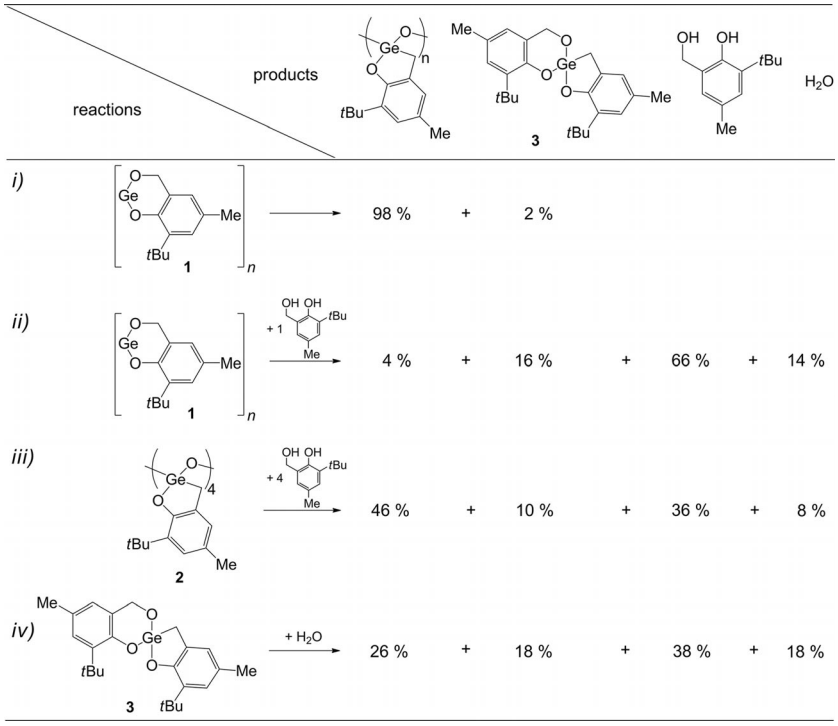

Scheme 2. Experiments monitored by ^{1}H NMR spectroscopy in [D_8]toluene for reactions (1)–(3) and $CDCl_3$ for reaction (4) with the final product ratios determined after 1) 190 h, 2) 185 h, 3) 16 min, and 4) 19 min.

A slow conversion of germylene **1** in the presence of 3-*tert*-butyl-2-hydroxy-5-methylbenzyl alcohol into germocane species such as **2** (4%) and **3** (16%) was observed in experiment ii) within 185 h (see Figure S5 in the Supporting Information). As the resonance signals assigned to germocane species and compound **3** increased in intensity, the intensities of the signals assigned to compound **1** and 3-*tert*-butyl-2-hydroxy-5-methylbenzyl alcohol decreased. Comparison of the intensities of the resonance signals centered at δ = 2.2 (CH_2Ge groups of germocanes and **3**) and 4.8 ppm (CH_2O groups of **3**) after different intervals of time indicated that the germocane species and compound **3** must be formed on similar timescales. Note, the ratio of 3-*tert*-butyl-2-hydroxy-5-methylbenzyl alcohol first decreased to 47% at 79 h and then increased continuously up to 66% after 185 h. In addition, resonance signals assigned to water appeared and increased steadily as the reaction mixture was monitored. The final mixture of experiment ii) consisted of germocane species (4%), compound **3** (16%), 3-*tert*-butyl-2-hydroxy-5-methylbenzyl alcohol (66%), and water (14%). Note that the addition of 2 equiv. of 3-*tert*-butyl-2-hydroxy-5-methylbenzyl alcohol qualitatively gave a similar progression of resonance signals and a final mixture of germocane species (2%), compound **3** (16%), 3-*tert*-butyl-2-hy-?>droxy-5-methylbenzyl alcohol (70%), and water (12%), which is indicative of an equilibrium (see the discussion below).

Germocane **2** reacted immediately to give **3** in the presence of 3-*tert*-butyl-2-hydroxy-5-methylbenzyl alcohol, as determined in experiment iii). The reaction mixture from experiment iii) consisted of germocane species (46%), compound **3** (10%), 3-*tert*-butyl-2-hydroxy-5-methylbenzyl alcohol (36%), and water (8%). It is noteworthy that the addition of 6 equiv. of 3-*tert*-butyl-2-hydroxy-5-methylbenzyl alcohol gave a mixture of germocane species (41%), compound **3** (12%), 3-*tert*-butyl-2-hydroxy-5-methylbenzyl alcohol (41%), and water (8%).

The spirocyclic germanium(IV) compound **3** was hydrolyzed in the presence of water with the simultaneous formation of germocanes, as observed in experiment iv). The reaction mixture consisted of germocane species (26%), compound **3** (18%), 3-*tert*-butyl-2-hydroxy-5-methylbenzyl alcohol (38%), and water (18%) after 19 min. The composition of the mixture was only marginally altered later on, which is again indicative of an equilibrium.

In summary, germylene **1** is converted into germocane species such as **2** in the absence of 3-*tert*-butyl-2-hydroxy-5-methylbenzyl alcohol. The formation of water was observed upon the conversion of either germylene **1** or germocane **2** into compound **3** in the presence of 3-*tert*-butyl-2-hydroxy-5-methylbenzyl alcohol, with germocane species remaining in the mixtures. In addition, the formation of germocanes was detected as compound **3** underwent hydrolysis. These observations may be explained as follows.

First, germocanes are initially formed by the slow conversion reaction of germylene **1**. Water is formed by the reaction of germocane species, for example, in the reaction of compound **2** with 3-*tert*-butyl-2-hydroxy-5-methylbenzyl alcohol to give compound **3** (Scheme 3, a).

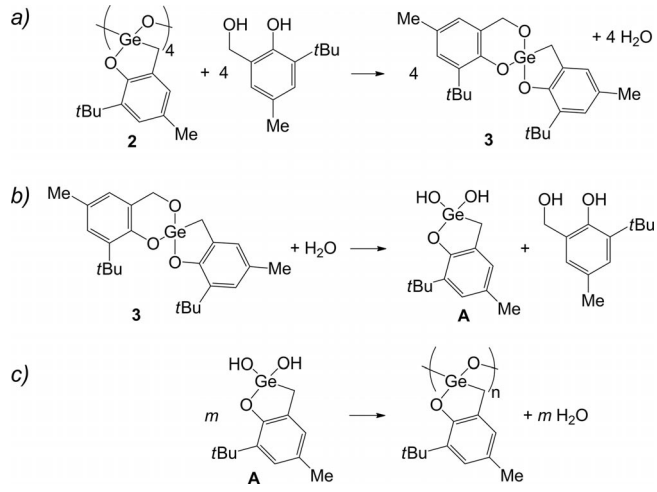

Scheme 3. Proposed reaction sequence for the formation of different germocane species. a) Reaction of **2** with 3-*tert*-butyl-2-hydroxy-5-methylbenzyl alcohol to form **3**, b) hydrolysis of **3** to give the oxagermolediol **A**, and c) condensation of **A** to give germocane species.

The generated water subsequently reacts with the germanium alcoholates [compounds **1** and **3** or at least **3** in the case of experiment iii), Scheme 3, b] by fast hydrolysis.[24] Thus, 3-*tert*-butyl-2-hydroxy-5-methylbenzyl alcohol is recovered, which explains the significantly larger proportion of 3-*tert*-butyl-2-hydroxy-5-methylbenzyl alcohol in the product ratios, even larger than in the initial reaction mixture of experiment ii). This is further supported by the observation that the content of 3-*tert*-butyl-2-hydroxy-5-methylbenzyl alcohol initially decreases, but recovers over the time of experiment ii). Moreover, the hydrolysis of **3** leads to 7-(*tert*-butyl)-5-methylbenzo[*d*][1,2]oxagermole-2,2(3*H*)-diol (**A**), which undergoes condensation to result again in the formation of germocane species (Scheme 3, c). Henceforward, these germocanes may also react with 3-*tert*-butyl-2-hydroxy-5-methylbenzyl alcohol to give compound **3**, causing equilibration between the reactions illustrated in Scheme 3. The latter is supported by the observation that repetitions of experiments ii) and iii) providing an excess of 3-*tert*-butyl-2-hydroxy-5-methylbenzyl alcohol led only to a modification of the ratios of the products but did not change the compositions of the final mixtures.

DFT-D Calculations

DFT-D calculations at the B3LYP-D3/def2-TZVPP level of theory were carried out to study the reactions of compound **1** to give **2**–**4**. The relative energies of **2**–**4** with respect to **1** and the proposed intermediates of two reaction paths that may explain the formation of the Ge–CH_2 bond and consequently the formation of compounds **2** and **3** starting from **1** were examined (Schemes 4, 5, and Table 1). It is assumed for reaction path I that monomeric **1** reacts to give a germanone (**B**) by intramolecular insertion (Scheme 5, a) to form the Ge–CH_2 bond. Then intermediate **B** reacts to give **2** or, in the presence of 3-*tert*-butyl-2-

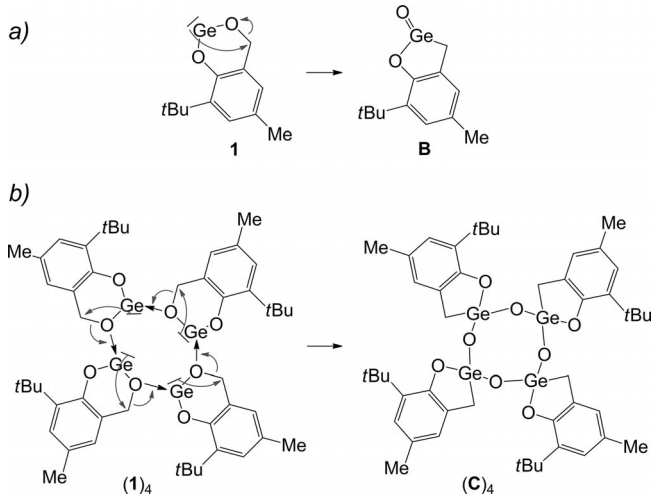

Scheme 4. Illustration of presumed rearrangement processes (blue arrows) that explain the formation of the Ge–CH_2 bond by intramolecular C–O insertion reaction of a) germylene **1** to give germanone **B** and b) $(\mathbf{1})_4$ to give germocane $(\mathbf{C})_4$ = **2**.

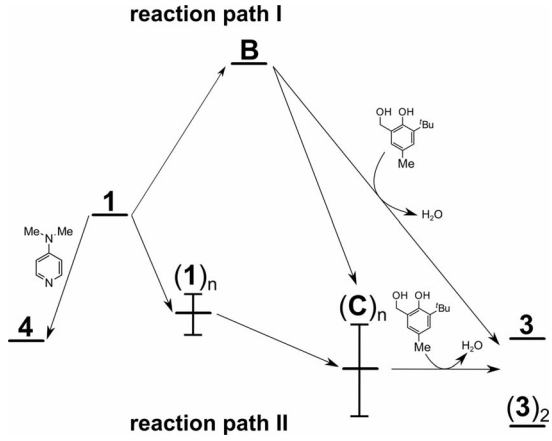

Scheme 5. Illustration of the proposed reaction paths with the relative energies of compounds **1**–**4**, the oligomers $(\mathbf{1})_n$ (n = 1–5), germanone **B**, species $(\mathbf{C})_n$ (n = 1–5; compound 2, n = 4), and the dimer $(\mathbf{3})_2$ calculated at the B3LYP-D3/def2-TZVPP level of theory to study the conversion of **1** into **2**–**4**.

Table 1. Relative energies (ΔE) and structures of compounds **1**–**4**, the oligomers $(\mathbf{1})_n$ (n = 1–5), germanone **B**, species $(\mathbf{C})_n$ (n = 1–5; compound **2**, n = 4), and the dimer $(\mathbf{3})_2$ calculated at the B3LYP-D3/def2-TZVPP level of theory.

Compd.	ΔE [kJ/mol]	Structure	Compd.	ΔE [kJ/mol]	Structure
1	0	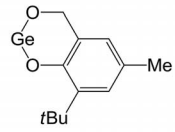	$(\mathbf{C})_n$	–77.5 (n = 2) –129.0 (n = 3) –139.8 (n = 4) –144.4 (n = 5)	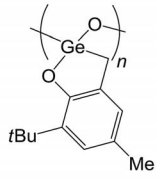
$(\mathbf{1})_n$	–55.9 (n = 2) –79.0 (n = 3) –85.5 (n = 4) –77.0 (n = 5)	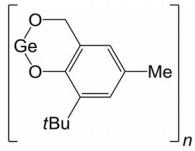	**3**	–89.3[a]	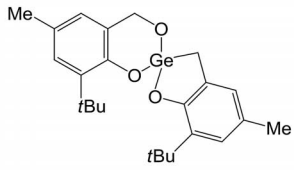
B	109.4	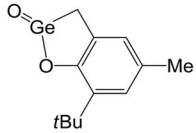	$(\mathbf{3})_2$	–152.5[a]	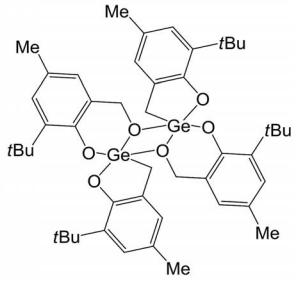
			4	–91.0[b]	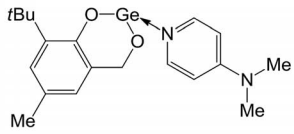

[a] Relative energies (ΔE) calculated by taking into account the total energies of 3-*tert*-butyl-2-hydroxy-5-methylbenzyl alcohol and water calculated at the B3LYP-D3/def2-TZVPP level of theory. [b] Relative energy (ΔE) calculated by taking into account the total energy of 4-(dimethylamino)pyridine calculated at the B3LYP-D3/def2-TZVPP level of theory.

hydroxy-5-methylbenzyl alcohol, **3**. It is assumed for reaction path II that monomeric **1** first oligomerizes to give $(\mathbf{1})_n$ (n = 1–5) before Ge–CH_2 bonds are formed by intramolecular insertion reactions [exemplarily shown in Scheme 4 (b) for the conversion of $(\mathbf{1})_4$ into $(\mathbf{C})_4$ = **2**] to result in species $(\mathbf{C})_n$ (n = 1–5). In the case of the conversion of **1** into **2**, no further reaction occurs [on the condition of tetramer formation, $(\mathbf{C})_4$ = **2**]. The formation of **3** is explained by the condensation of species $(\mathbf{C})_n$ with 3-*tert*-butyl-2-hydroxy-5-methylbenzyl alcohol.

The calculated formation energy of the intermediate **B** is endothermic by 109.4 kJ mol^{-1} (reaction path I), probably due to the formation of an unfavorable Ge=O bond.[25] In contrast, the reaction steps of reaction path II are all energetically favored (Scheme 4 and Table 1). Therefore, we suppose that reaction path I can be ruled out. In the case of the first reaction step of reaction path II, the formation of the tetramer $(\mathbf{1})_4$ (–85.5 kJ mol^{-1}) was found to be energetically favored in comparison with the formation of the dimer $(\mathbf{1})_2$ (–55.9 kJ mol^{-1}), trimer $(\mathbf{1})_3$ (–79.0 kJ mol^{-1}), and pentamer $(\mathbf{1})_5$ (–77.0 kJ mol^{-1}). Note, the small energy differences between the oligomers $(\mathbf{1})_n$ indicate that they may be in chemical equilibrium in the solution phase. The equilibrium between the oligomers $(\mathbf{1})_n$ may depend on the specific conditions of the solution (e.g., polarity of the solvent and/or temperature). We assume that at least the tetramer $(\mathbf{1})_4$ rather than the dimer $(\mathbf{1})_2$ is in equilibrium with the trimer $(\mathbf{1})_3$ in $CDCl_3$ solution based on our experimental results (see above). Following reaction path II, the conversions of the oligomers $(\mathbf{1})_n$ into $(\mathbf{C})_n$ exhibiting Ge–CH_2 bonds are exothermic. Species $(\mathbf{C})_5$ (–144.4 kJ mol^{-1}) was calculated to be the energetically slightly favored species. However, $(\mathbf{C})_4$ (–139.8 kJ mol^{-1}) is similar in energy and was obtained experimentally [$(\mathbf{C})_4$ ≙ germocane **2**]. Please note that this contradiction may be easily comprehensible bearing in mind the level of theory applied. An estimate of the uncertainty in the calculated energies easily amounts to 5–10 kJ mol^{-1}, as the results were obtained by using DFT methods and furthermore do not include the influence of solvent. In addition, the conversion of tetramer $(\mathbf{1})_4$ into $(\mathbf{C})_4$ by intramolecular oxidative insertion reactions may have lower reaction barriers in comparison with the conversion reactions of other oligomers [e.g., $(\mathbf{1})_5 \rightarrow (\mathbf{C})_5$], which may kinetically favor the formation of germocane $(\mathbf{C})_4$. The reaction of $(\mathbf{C})_4$ (–139.8 kJ mol^{-1}) with 3-*tert*-butyl-2-hydroxy-5-methylbenzyl alcohol to give monomeric **3** (–89.3 kJ mol^{-1}) is endothermic, but if the dimerization of **3** to give $(\mathbf{3})_2$, as is observed in solution and in the solid state (see above) is taken into account, the conversion of $(\mathbf{C})_4$ into **3** is energetically favorable. Thus, reaction path II is in agreement with our experimental results. It is also worth noting that the energy of compound **4** was calculated to be –91.0 kJ mol^{-1}. Hence, the formation of complex **4** upon intermolecular donor stabilization is energetically favored compared with the oligomerization of **1** and thus prohibits the conversion of the germylene **1** into the germocane $(\mathbf{C})_4$, in accordance with experimental results, at least at ambient temperature. In addition, the decomposition of complex **4** upon heating into 4-(dimethylamino)pyridine and germylene **1**, which may further react to give germocane $(\mathbf{C})_4$, as determined experimentally (see above), is quite likely in view of its moderate energy of formation (–91.0 kJ mol^{-1}).

Conclusions

The first representative of an unsymmetrical cyclic germylene possessing both an aryloxide as well as an alkoxide moiety as part of a heterocycle, namely germanium(II) 2-*tert*-butyl-4-methyl-6-(oxidomethyl)phenolate (**1**), has been reported herein. The germylene **1** is not stable in solution and converts into a cyclic germanium(IV) compound, 2,4,6,8-tetrakis(3-*tert*-butyl-5-methyl-2-oxidophenyl)methanide-1,3,5,7,2,4,6,8-tetraoxidogermocane (**2**), by intramolecular insertion of germanium into the benzylic C–O bond to form a Ge–CH_2 bond. In the presence of 3-*tert*-butyl-2-hydroxy-5-methylbenzyl alcohol, the spirocyclic germanium(IV) compound, 7,8′-di-*tert*-butyl-5,6′-dimethyl-3*H*,4′*H*-spiro[benzo[*d*][1,2]oxagermole-2,2′-benzo[*d*][1,3,2]-dioxagermine] (**3**), was obtained starting from either germylene **1** or germocane **2**. Compound **3**, which exhibits a Ge–CH_2 bond in its molecular structure, is a condensation product of germocane **2** with 3-*tert*-butyl-2-hydroxy-5-methylbenzyl alcohol. Experimental studies and DFT-D calculations were carried out to account for the formation of germocane **2** and spirocyclic **3** starting from germylene **1**. Based on our results, we suggest the following. 1) Compound **1** forms oligomers with $(\mathbf{1})_3$ being the major species in chemical equilibrium in solution. 2) Intramolecular insertion reactions of the oligomers $(\mathbf{1})_n$ slowly lead to cyclic germocane species in solution with the formation of a tetranuclear cyclic germocane –[Ge–O]$_4$– species (**2**) favored. 3) The formation of –[Ge–O]$_4$– (**2**) requires the intermediate formation of $(\mathbf{1})_4$, which is a minor species in solution. 4) In the presence of 3-*tert*-butyl-2-hydroxy-5-methylbenzyl alcohol, germocane **2** reacts by a condensation reaction with the alcohol to give the spirocyclic compound **3**. 5) Intermolecular donor stabilization of germylene **1** upon addition of 4-(dimethylamino)pyridine prohibits oligomerization and thus the conversion reaction, at least at ambient temperature, as a result of the formation of the stable 1:1 complex **4**. In conclusion, a novel, highly reactive germylene has been accessed that shows unprecedented intramolecular C–O insertion of germanium(II). The resulting monoorgano germocane is prone to condensation reactions with 3-*tert*-butyl-2-hydroxy-5-methylbenzyl alcohol, finally resulting in equilibration between germocanes, monoorgano germanium alkoxides, 3-*tert*-butyl-2-hydroxy-5-methylbenzyl alcohol, and water. Similar reactivity might be expected for other salicyl alcoholates with elements in their low-valent state.

Experimental Section

General: All reactions were performed under argon using Schlenk techniques or in a glovebox. Solvents were purified and dried by

applying standard techniques prior to use. All reactions were carried out with freshly distilled, dried solvents. Experiments involving freshly activated molecular sieves were performed without stirring. ^{1}H, ^{13}C{^{1}H}, and ^{1}H–^{13}C{^{1}H} HSQC NMR spectra were recorded with a Bruker Avance III 500 spectrometer. $CDCl_3$ was dried with molecular sieves. ^{1}H NMR spectroscopic studies were carried out under inert conditions in sealed NMR tubes using either freshly prepared [D_8]toluene dried with potassium or $CDCl_3$. ^{1}H NMR spectra were recorded after preparation and at reasonable intervals. ATR-FTIR spectra were recorded with a BioRad FTS-165 spectrometer. Melting points were determined with a B-540 melting point apparatus from Büchi. CHN analyses were determined by using a FlashEA 1112 NC Analyzer from Thermo Fisher Scientific. DSC experiments were determined with a Mettler Toledo DSC 30 instrument using 40 μL aluminium crucibles. The measurements were taken up to 400 °C at a heating rate of 10 K min^{-1} in N_2 and at a volume flow of 50 mL min^{-1}. TGA/DSC experiments were determined with a Mettler Toledo TGA/DSC1 1600 system with an MX1 balance in the range of 40–800 °C at a heating rate of 10 K min^{-1} in Ar and at a volume flow of 60 mL min^{-1}.

Germanium(IV) chloride and 1,1,1,3,3,3-hexamethyldisilazane were purchased from ABCR GmbH & Co KG. *n*-Butyllithium (2.5 M) and 2-*tert*-butyl-4-methylphenol were purchased from Merck Schuchardt OHG and Thermo Fisher Scientific, respectively. 4-(Dimethylamino)pyridine was purchased from Alfa Aesar GmbH & Co KG. 3-*tert*-Butyl-2-hydroxy-5-methylbenzyl alcohol,[26] $GeCl_2$·1,4-dioxane,[27] $LiN(SiMe_3)_2$,[27] and $Ge[N(SiMe_3)_2]_2$[1] were synthesized according to literature procedures.

Germanium(II) 2-*tert*-Butyl-4-methyl-6-(oxidomethyl)phenolate (1): A solution of 3-*tert*-butyl-2-hydroxy-5-methylbenzyl alcohol (318.0 mg, 1.638 mmol) in *n*-pentane (7 mL) was added dropwise to a solution of $Ge[N(SiMe_3)_2]_2$ (644.0 mg, 1.638 mmol) in *n*-pentane (5 mL) at ambient temperature. The pale-yellow solution was stirred for 10 min. The volatile solvent (approximately 4/5 of the solvent volume) was removed by slow evaporation under reduced pressure (10^{-1} mbar). A colorless precipitate was formed during evaporation of the solvent. The colorless solid was filtered off and washed with *n*-pentane (thrice with 1 mL each) to give compound **1** after evaporating all volatile residues under reduced pressure (10^{-2} mbar), yield 361.0 mg, 83%. TGA, DSC, and melting-point determination (see Figures S3 and S4 in the Supporting Information) revealed that compound **1** decomposes at 133 °C by an exothermic process. ^{1}H NMR (500 MHz, $CDCl_3$, 25 °C, TMS): δ = 1.36 (s, 9 H, *t*Bu), 1.44 (s, 9 H, *t*Bu), 1.45 (s, 9 H, *t*Bu), 2.19 (s, 3 H, Me), 2.23 (s, 3 H, Me), 2.33 (s, 3 H, Me), 4.28 (d, $^2J_{CH2}$ = 12.6 Hz, 1 H, H_A/CH_2), 4.31 (d, $^2J_{CH2}$ = 12.6 Hz, 1 H, H_B/CH_2), 4.40 (d, $^2J_{CH2}$ = 12.0 Hz, 1 H, $H_{A'}$/CH_2), 4.46 (d, $^2J_{CH2}$ = 12.6 Hz, 1 H, $H_{A''}$/CH_2), 4.57 (d, $^2J_{CH2}$ = 12.6 Hz, 1 H, $H_{B''}$/CH_2), 4.73 (d, $^2J_{CH2}$ = 12.0 Hz, 1 H, $H_{B'}$/CH_2), 5.82 (d, $^4J_{meta}$ = 1.3 Hz, 1 H, C_6H_2), 6.66 (d, $^4J_{meta}$ = 1.0 Hz, 1 H, C_6H_2), 6.75 (d, $^4J_{meta}$ = 1.3 Hz, 1 H, C_6H_2), 7.05 (d, $^4J_{meta}$ = 1.0 Hz, 1 H, C_6H_2), 7.07 (d, $^4J_{meta}$ = 1.3 Hz, 1 H, C_6H_2), 7.15 (d, $^4J_{meta}$ = 1.3 Hz, 1 H, C_6H_2) ppm. ^{13}C{^{1}H} NMR (125 MHz, $CDCl_3$, 25 °C, TMS): δ = 20.9 (Me), 29.8 (C_p, *t*Bu), 30.0 (C_p, *t*Bu), 30.1 (C_p, *t*Bu), 128.5 (C_6H_2) ppm. ^{1}H–^{13}C{^{1}H} HSQC NMR (125 MHz, $CDCl_3$, 25 °C, TMS): δ = 1.28/29.9 (*t*Bu), 1.30/29.3 (*t*Bu), 1.37/29.8 (*t*Bu), 2.15/20.7 (Me), 2.22/20.8 (Me), 2.25/20.8 (Me), 4.22/61.9 (CH_2), 4.32/61.8 (CH_2), 4.38/63.5 (CH_2), 4.49/63.7 (CH_2), 4.64/61.8 (CH_2), 5.74/127.2 (C_6H_2), 6.58/126.5 (C_6H_2), 6.66/126.2 (C_6H_2), 6.97/128.5 (C_6H_2), 6.99/128.9 (C_6H_2), 7.07/128.5 (C_6H_2) ppm. FTIR (ATR): $\tilde{\nu}$ = 3021 (ν C_{aryl}–H), 2946 (ν CH_3/CH_2), 2909 (ν CH_3/CH_2), 2859 (ν CH_3/CH_2), 1607 (ν C=C), 1470 (δ CH_3), 1441 (δ CH_3/CH_2), 1225 (ν C–O), 1153 (ν C–C), 864, 815, 797 (δ C_{aryl}–H, C_6H_2 backbone vibrations), 677, 602 (ν Ge–O), 556 (O–Ge–O) cm^{-1}. $C_{12}H_{16}GeO_2$ (264.85): calcd. C 54.41, H 6.09; found C 53.91, H 6.55. Single crystals suitable for X-ray diffraction analysis were obtained by evaporation of a saturated solution of compound **1** in diethyl ether within 1 hour at ambient temperature.

2,4,6,8-Tetrakis(3-*tert*-butyl-5-methyl-2-oxidophenyl)methanide-1,3,5,7,2,4,6,8-tetraoxidogermocane (2)

Method a: A solution of germylene **1** (23.0 mg, 8.68×10^{-2} mmol) in 1,4-dioxane (5 mL) was stirred at ambient temperature for 30 min. Colorless crystals of [**2**·$(C_4H_8O_2)_2$]·$3C_4H_8O_2$ were filtered off after 2 weeks. These crystals were used for X-ray diffraction analysis. Removal of the residual solvent of the filtrate under reduced pressure (10^{-2} mbar) gave [**2**·$(C_4H_8O_2)_2$] as a colorless solid, yield 18.4 mg, 80%; m.p. 159–167 °C (decomp. at ca. 250 °C). ^{1}H NMR (500 MHz, $CDCl_3$, 25 °C, TMS): δ = 1.38 (s, 9 H, *t*Bu), 1.41 (s, 9 H, *t*Bu), 1.42 (s, 9 H, *t*Bu), 1.43 (s, 9 H, *t*Bu), 2.22 (s, 3 H, Me), 2.23 (s, 3 H, Me), 2.24 (s, 3 H, Me), 2.24 (s, 3 H, Me), 2.46–2.62 (m, 8 H, CH_2), 3.70 (s, 16 H, CH_2, 1,4-dioxane), 6.93 (d, $^4J_{meta}$ = 0.6 Hz, 4 H, C_6H_2), 6.94 (d, $^4J_{meta}$ = 0.6 Hz, 4 H, C_6H_2) ppm. ^{13}C{^{1}H} NMR (125 MHz, $CDCl_3$, 25 °C, TMS): δ = 15.3 (CH_2), 20.9 (Me), 29.5 (C_p, *t*Bu), 34.8 (C_q, *t*Bu), 67.1 (CH_2, 1,4-dioxane), 121.5 (C_6H_2), 126.3 (C_6H_2), 126.9 (C_6H_2), 128.5 (C_6H_2), 136.1 (C_6H_2), 153.8 (C_6H_2) ppm. ^{1}H–^{13}C{^{1}H} HSQC NMR (125 MHz, $CDCl_3$, 25 °C, TMS): δ = 1.23/29.3 (C_p, *t*Bu), 1.26/29.4 (C_p, *t*Bu), 1.30/29.4 (C_p, *t*Bu), 1.35/29.3 (C_p, *t*Bu), 2.44/15.5 (CH_2), 2.50/15.0 (CH_2), 2.54/15.2 (CH_2), 2.16/20.8 (Me), 3.63/67.0 (CH_2, 1,4-dioxane), 6.81/126.6 (C_6H_2), 6.85/126.3 (C_6H_2) ppm. FTIR (ATR): $\tilde{\nu}$ = 3023 (ν C_{aryl}–H), 2967 (ν CH_3/CH_2), 2923 (ν CH_3/CH_2), 2857 (ν CH_3/CH_2), 1636 (ν C=C), 1492 (δ CH_3), 1391 (δ CH_3/CH_2), 1248 (ν C–O), 1221 (ν C–O), 1134 (ν C–C), 1086 (ν C–C), 853, 830, 808 (δ C_{aryl}–H and C_6H_2 backbone vibrations), 658, 602 (ν Ge–O), 532(ν Ge–C) cm^{-1}. $C_{56}H_{80}Ge_4O_{12}$, [**2**·$(C_4H_8O_2)_2$] (1235.68): calcd. C 54.43, H 6.53; found C 54.25, H 6.62.

Method b: A solution of compound **1** (438.4 mg, 1.655 mmol) in diethyl ether (45 mL) was stirred at ambient temperature for 132 h. Removal of all volatiles under reduced pressure (10^{-2} mbar) yielded a colorless solid (311.7 mg). The product was composed of compound **2** (88%; yield 0.278 mmol, 67%) and compound **3** (12%; yield 0.038 mmol, 9%), as determined by ^{1}H NMR analysis.

7,8′-Di-*tert*-butyl-5,6′-dimethyl-3*H*,4′*H*-spiro[benzo[*d*][1,2]oxagermole-2,2′-benzo[*d*][1,3,2]dioxagermine] (3)

Method a: A solution of germylene **1** (249.8 mg, 0.9431 mmol) in 1,4-dioxane (50 mL) was heated at reflux with stirring for 21 h. Removal of the solvent under reduced pressure (10^{-2} mbar) at 50 °C gave a colorless solid. The product was suspended in diethyl ether (10 mL) and insoluble byproducts were removed by filtration. Compound **3** was obtained after removal of all volatiles under reduced pressure (10^{-2} mbar), yield 50.0 mg, 24.0%; m.p. 213–216 °C. ^{1}H NMR (500 MHz, $CDCl_3$, 25 °C, TMS): δ = 1.36 (s, 18 H, *t*Bu), 2.27 (s, 3 H, Me), 2.30 (s, 3 H, Me), 2.59 (d, $^2J_{CH2}$ = 17.6 Hz, 1 H, $H_{A'}$/CH_2Ge), 2.64 (d, $^2J_{CH2}$ = 17.6 Hz, 1 H, $H_{B'}$/CH_2Ge), 5.04 (d, $^2J_{CH2}$ = 13.1 Hz, 1 H, $H_{X'}$/CH_2O), 5.12 (d, $^2J_{CH2}$ = 13.1 Hz, 1 H, $H_{Y'}$/CH_2O), 6.78 (d, $^4J_{meta}$ = 1.9 Hz, 1 H, C_6H_2), 6.96 (d, $^4J_{meta}$ = 1.3 Hz, 1 H, C_6H_2), 6.98 (d, $^4J_{meta}$ = 1.3 Hz, 1 H, C_6H_2), 7.09 (d, $^4J_{meta}$ = 1.9 Hz, 1 H, C_6H_2) ppm. ^{13}C{^{1}H} NMR (125 MHz, $CDCl_3$, 25 °C, TMS): δ = 13.1 (CH_2Ge), 20.8 (Me), 20.9 (Me), 29.4 (C_p, *t*Bu), 29.8 (C_p, *t*Bu), 34.7 (C_q, *t*Bu), 34.8 (C_q, *t*Bu), 67.2 (CH_2O), 121.4 (C_6H_2), 126.0 (C_6H_2), 126.4 (C_6H_2), 126.9 (C_6H_2), 127.7 (C_6H_2), 128.5 (C_6H_2), 128.7 (C_6H_2), 130.2 (C_6H_2), 136.6 (C_6H_2), 139.6 (C_6H_2), 151.9 (C_6H_2), 153.8 (C_6H_2) ppm. ^{1}H–^{13}C{^{1}H} HSQC NMR (125 MHz, $CDCl_3$, 25 °C, TMS): δ = 1.29/

29.4 (*t*Bu), 2.19/20.7 (Me), 2.22/20.7 (Me), 2.54/12.8 (CH_2Ge), 4.98/67.0 (CH_2O), 5.03/67.0 (CH_2O), 6.70/126.0 (C_6H_2), 6.88/126.4 (C_6H_2), 6.90/126.5 (C_6H_2), 7.01/127.5 (C_6H_2) ppm. NMR analysis data for (**3**)$_2$: ^{1}H NMR (500 MHz, $CDCl_3$, 25 °C, TMS): δ = 0.83 (d, $^2J_{CH2}$ = 17.6 Hz, 1 H, H_A/CH_2), 1.48 (s, 9 H, *t*Bu), 1.53 (s, 9 H, *t*Bu), 1.80 (s, 3 H, Me), 2.24 (s, 3 H, Me), 2.32 (d, $^2J_{CH2}$ = 17.6 Hz, 1 H, H_B/CH_2), 4.72 (d, $^2J_{CH2}$ = 12.6 Hz, 1 H, $H_{A'}$/CH_2), 4.99 (d, $^2J_{CH2}$ = 12.6 Hz, 1 H, $H_{B'}$/CH_2), 5.90 (s, 1 H, C_6H_2), 6.65 (s, 1 H, C_6H_2), 6.92 (s, 1 H, C_6H_2), 7.06 (s, 1 H, C_6H_2) ppm. ^{13}C{^{1}H} NMR (125 MHz, $CDCl_3$, 25 °C, TMS): δ = 16.0 (CH_2), 20.4 (Me), 20.9 (Me), 29.6 (C_p, *t*Bu), 29.8 (C_p, *t*Bu), 34.8 (C_q, *t*Bu), 34.9 (C_q, *t*Bu), 66.8 (CH_2O), 121.7 (C_6H_2), 125.4 (C_6H_2), 126.1 (C_6H_2), 126.4 (C_6H_2), 127.2 (C_6H_2), 127.5 (C_6H_2), 128.6 (C_6H_2), 130.4 (C_6H_2), 135.1 (C_6H_2), 141.2 (C_6H_2), 152.8 (C_6H_2), 153.7 (C_6H_2) ppm. ^{1}H–^{13}C{^{1}H} HSQC NMR (125 MHz, $CDCl_3$, 25 °C, TMS): δ = 0.74/15.8 (CH_2), 1.41/29.3 (*t*Bu), 1.45/29.4 (*t*Bu), 1.73/20.1 (Me), 2.16/20.7 (Me), 2.22/15.8 (CH_2), 4.62/66.7 (CH_2O), 4.90/66.7 (CH_2O), 5.82/127.0 (C_6H_2), 6.57/126.1 (C_6H_2), 6.85/125.2 (C_6H_2), 6.97/127.4 (C_6H_2) ppm. FTIR (ATR): $\tilde{\nu}$ = 3012 (ν C_{aryl}–H), 2965 (ν CH_3/CH_2), 2944 (ν CH_3/CH_2), 2909 (ν CH_3/CH_2), 2863 (ν CH_3/CH_2), 1607 (ν C=C), 1466 (δ CH_3), 1439 (δ CH_3/CH_2), 1227 (ν C–O), 978 (ν C–C), 940 (ν C–C), 862, 841, 808 (δ C_{aryl}–H and C_6H_2 backbone vibrations), 673, 617 (ν Ge–O), 575, 542 (ν Ge–C) cm^{-1}. $C_{24}H_{32}Ge_2O_6$ (561.69): calcd. C 65.34, H 7.31; found C 64.95, H 7.45. Single crystals of (**3**)$_2$ suitable for X-ray diffraction analysis were obtained by crystallization from 1,4-dioxane/CH_2Cl_2 solution.

Method b: A solution of germylene **1** (100.0 mg, 0.3775 mmol) and 3-*tert*-butyl-2-hydroxy-5-methylbenzyl alcohol (73.3 mg, 0.3775 mmol) in diethyl ether (21 mL) was prepared in a Schlenk tube equipped with freshly activated molecular sieves at ambient temperature. The mixture was aged for 159 h. A precipitate formed that was dissolved by the addition of THF. Filtration and removal of the solvent under reduced pressure (10^{-2} mbar) gave a colorless solid (128.8 mg). The product was composed of compound **3** (81%; yield 0.265 mmol, 70%) and 3-*tert*-butyl-2-hydroxy-5-methylbenzyl alcohol (19%; yield 0.062 mmol), as determined by ^{1}H NMR analysis.

Method c: A solution of germocane **2** (8.3 mg, 7.8×10^{-3} mmol) and 3-*tert*-butyl-2-hydroxy-5-methylbenzyl alcohol (6.1 mg, 3.13×10^{-2} mmol) in diethyl ether (15 mL) was prepared in a Schlenk tube equipped with freshly activated molecular sieves at ambient temperature and allowed to age for 2 d. Filtration and removal of the solvent under reduced pressure (10^{-2} mbar) yielded a colorless solid (6.1 mg). The product was composed of compound **3** (87%; yield 1.30×10^{-2} mmol, 41%) and 3-*tert*-butyl-2-hydroxy-5-methylbenzyl alcohol (13%; 1.9×10^{-3} mmol) as determined by ^{1}H NMR analysis.

[4-(Dimethylamino)pyridine][germanium(II) 2-*tert*-Butyl-4-methyl-6-(oxidomethyl)phenolate] (4): A solution of germylene **1** (292.3 mg, 1.104 mmol) and 4-(dimethylamino)pyridine (134.8 mg, 1.104 mmol) in diethyl ether (30 mL) was stirred at ambient temperature for 16 h. Removal of the solvent under reduced pressure (10^{-2} mbar) gave a colorless solid that was washed with *n*-pentane (3 × 3 mL) to give the germylene complex **4** as a colorless solid after evaporating volatile residues under reduced pressure (10^{-2} mbar), yield 322.9 mg, 75%; m.p. 143–145 °C. ^{1}H NMR (500 MHz, $CDCl_3$, 25 °C, TMS): δ = 1.40 (s, 9 H, *t*Bu), 2.25 (s, 3 H, Me), 3.07 (s, 6 H, Me), 4.48 (s, 2 H, CH_2), 6.52 (dd, $^3J_{ortho}$ = 5.7, $^4J_{meta}$ = 1.6 Hz, 2 H, C_5H_4N), 6.70 (s, $^4J_{meta}$ = 2.2 Hz, 1 H, C_6H_2), 7.01 (d, $^4J_{meta}$ = 2.2 Hz, 1 H, C_6H_2), 8.14 (dd, $^3J_{ortho}$ = 5.7, $^4J_{meta}$ = 1.6 Hz, 2 H, C_5H_4N) ppm. ^{13}C{^{1}H} NMR (125 MHz, $CDCl_3$, 25 °C, TMS): δ = 20.8 (Me), 29.8 (C_p, *t*Bu), 34.6 (C_q, *t*Bu), 39.3 (Me), 63.1 (CH_2), 106.6 (C_5H_4N), 125.8 (C_6H_2), 126.1 (C_6H_2), 126.4 (C_6H_2), 131.3 (C_6H_2), 138.6 (C_6H_2), 145.5 (C_5H_4N), 152.8 (C_5H_4N), 155.7 (C_6H_2) ppm. ^{1}H–^{13}C{^{1}H} HSQC NMR (125 MHz, $CDCl_3$, 25 °C, TMS): δ = 1.32/29.4 (*t*Bu), 2.18/20.8 (Me), 3.00/39.3 (Me), 4.41/62.8 (CH_2), 6.46/106.2 (C_5H_4N), 6.63/126.1 (C_6H_2), 6.95/126.1 (C_6H_2), 8.08/144.2 (C_5H_4N) ppm. FTIR (ATR): $\tilde{\nu}$ = 3068 (ν C_{aryl}–H), 2994 (ν C_{aryl}–H), 2956 (ν CH_3/CH_2), 2906 (ν CH_3/CH_2), 2857 (ν CH_3/CH_2), 2834 (ν CH_3/CH_2), 1619 (ν C=C/C=N), 1536 (ν C=C/C=N), 1462 (δ = CH_3), 1439 (δ CH_3/CH_2), 1391 (ν C_{aryl}–N), 1244 (ν C–O), 1217 (ν C–N), 1150 (ν C–C), 860, 843, 808 (δ C_{aryl}–H and C_6H_2 backbone vibrations), 606, 569 (ν Ge–O), 540(ν Ge–N) cm^{-1}. $C_{19}H_{26}GeN_2O_2$ (387.02): calcd. C 58.96, H 6.77, N 7.24; found C 58.49, H 6.77, N 7.12. Single crystals suitable for X-ray diffraction analysis were obtained by slow evaporation of the solvent at ambient temperature of a saturated solution of complex **4** in diethyl ether.

^{1}H NMR Spectroscopic Study i): Compound **1** (9.8 mg, 3.7×10^{-2} mmol) was dissolved in [D_8]toluene (0.5 mL). The solution was stored under inert conditions in a sealed NMR tube at ambient temperature. ^{1}H NMR spectra were recorded within 237 h of preparation. The composition of the mixture did not change after 190 h. The final mixture consisted of germocane species (98%) and compound **3** (2%), as determined by ^{1}H NMR analysis.

^{1}H NMR Spectroscopic Study ii)

Method a: A mixture of compound **1** (8.0 mg, 3.0×10^{-2} mmol) and 3-*tert*-butyl-2-hydroxy-5-methylbenzyl alcohol (5.8 mg, 3.0×10^{-2} mmol) was dissolved in [D_8]toluene (0.5 mL). The solution was stored under inert conditions in a sealed NMR tube at ambient temperature. ^{1}H NMR spectra were recorded within 231 h of preparation. The composition of the mixture did not change after 185 h. The final mixture consisted of germocane species (4%), compound **3** (16%), 3-*tert*-butyl-2-hydroxy-5-methylbenzyl alcohol (66%), and water (14%), as determined by ^{1}H NMR analysis.

Method b: A mixture of compound **1** (4.2 mg, 1.6×10^{-2} mmol) and 3-*tert*-butyl-2-hydroxy-5-methylbenzyl alcohol (6.2 mg, 3.2×10^{-2} mmol) was dissolved in [D_8]toluene (0.5 mL). The solution was stored under inert conditions in a sealed NMR tube at ambient temperature. ^{1}H NMR spectra were recorded within 231 h of preparation. The composition of the mixture did not change after 185 h. The final mixture consisted of germocane species (2%), compound **3** (16%), 3-*tert*-butyl-2-hydroxy-5-methylbenzyl alcohol (70%), and water (12%), as determined by ^{1}H NMR analysis.

^{1}H NMR Spectroscopic Study iii)

Method a: A mixture of compound **2** (6.1 mg, 5×10^{-3} mmol) and 3-*tert*-butyl-2-hydroxy-5-methylbenzyl alcohol (4.2 mg, 2.2×10^{-2} mmol) was dissolved in [D_8]toluene (0.5 mL). The solution was stored under inert conditions in a sealed NMR tube at ambient temperature. ^{1}H NMR spectra were recorded within 137 h of preparation. The composition of the mixture did not change after its first analysis by ^{1}H NMR spectroscopy within 16 min of preparation. The final mixture consisted of germocane species (46%), compound **3** (10%), 3-*tert*-butyl-2-hydroxy-5-methylbenzyl alcohol (36%), and water (8%), as determined by ^{1}H NMR analysis.

Method b: A mixture of compound **2** (4.9 mg, 4×10^{-3} mmol) and 3-*tert*-butyl-2-hydroxy-5-methylbenzyl alcohol (4.6 mg, 2.4×10^{-2} mmol) was dissolved in [D_8]toluene (0.5 mL). The solution was stored under inert conditions in a sealed NMR tube at ambient temperature. ^{1}H NMR spectra were recorded within 137 h of preparation. The composition of the mixture did not change

after its first analysis by ^{1}H NMR spectroscopy within 15 min of preparation. The final mixture consisted of germocane species (41%), compound **3** (12%), 3-*tert*-butyl-2-hydroxy-5-methylbenzyl alcohol (39%), and water (8%), as determined by ^{1}H NMR analysis.

^{1}H NMR Spectroscopic Study iv): Compound **3** (14.0 mg, 3.1×10^{-2} mmol) was dissolved in water-saturated $CDCl_3$ (0.5 mL). The solution was stored under inert conditions in a sealed NMR tube at ambient temperature. ^{1}H NMR spectra were recorded within 121 h of preparation. The composition of the mixture did not change after its first analysis by ^{1}H NMR spectroscopy within 19 min of preparation. The final mixture consisted of germocane species (26%), compound **3** (18%), 3-*tert*-butyl-2-hydroxy-5-methylbenzyl alcohol (38%), and water (18%), as determined by ^{1}H NMR analysis.

^{1}H NMR Spectroscopic Study of the Mixture of Complex 4 and 3-*tert*-Butyl-2-hydroxy-5-methylbenzyl Alcohol in $CDCl_3$: A mixture of compound **4** (5.1 mg, 1.3×10^{-2} mmol) and 3-*tert*-butyl-2-hydroxy-5-methylbenzyl alcohol (2.6 mg, 1.3×10^{-2} mmol) was dissolved in $CDCl_3$ (0.5 mL). ^{1}H NMR spectra were recorded of the freshly prepared solution as well as of the solution stored under inert conditions and at ambient temperature within 48 h of preparation. All recorded ^{1}H NMR spectra were identical by their chemical shifts as well as their intensities of resonance signals, which indicating that compound **4** does not undergo any reaction with 3-*tert*-butyl-2-hydroxy-5-methylbenzyl alcohol.

^{1}H NMR Spectroscopic Study of Complex 4 in $CDCl_3$ at Elevated Temperature: Compound **4** (6.4 mg, 1.7×10^{-2} mmol) was dissolved in $CDCl_3$ (0.5 mL). ^{1}H NMR spectra were recorded of the freshly prepared solution and after heating the solution at 60 °C for 6 h. The solution was not stored under an inert atmosphere during heating. ^{1}H NMR spectroscopic analysis of the solution after 6 h revealed a composition of germocane species (5%), compound **3** (28%) and the complex **4** (67%).

Reaction of Complex 4 at Elevated Temperature: Complex **4** (171.4 mg, 4.42×10^{-1} mmol) was dissolved in toluene (50 mL) and stirred at 100 °C for 23 h. Removal of the solvent under reduced pressure (10^{-2} mbar) yielded a colorless solid. The product was composed of germocane species (10%), compound **3** (3%), and 4-(dimethylamino)pyridine (87%), as determined by ^{1}H NMR analysis. Note that the product should theoretically consist of germocane **2** (20%) and 4-(dimethylamino)pyridine (80%), respectively, if clean conversion of complex **4** into germocane **2** and 4-(dimethylamino)pyridine is assumed.

Single-Crystal X-ray Diffraction Analyses: Crystallographic data of $(\mathbf{1})_3 \cdot Et_2O$, $[\mathbf{2} \cdot (C_4H_8O_2)_2] \cdot 3C_4H_8O_2$, $(\mathbf{3})_2$, and **4** were collected with an Oxford Gemini S diffractometer (CrysAlis RED Version 1.171.32.5 from Oxford Diffraction Ltd.) by using Mo-K_α (λ = 0.71073 Å) or Cu-K_α radiation (λ = 1.54184 Å) at 100 or 110 K. The structures were solved by direct methods using SHELXS-2013 and refined by full-matrix least-square procedures on F^2 using SHELXL-2013.[28] Absorption corrections were semi-empirical from equivalents. All non-hydrogen atoms were refined anisotropically and a riding model was employed in the refinement of hydrogen atom positions. The crystallographic data are presented in Table 2.

CCDC-1057425 [for $2(\mathbf{1})_3 \cdot Et_2O$], -1057424 {for $[\mathbf{2} \cdot (C_4H_8O_2)_2] \cdot 3C_4H_8O_2$}, -1056308 [for $(\mathbf{3})_2$], and -1057426 (for **4**) contain the

Table 2. Crystallographic and experimental data of the single-crystal X-ray diffraction analyses of $2(\mathbf{1})_3 \cdot Et_2O$, $[\mathbf{2} \cdot (C_4H_8O_2)_2] \cdot 3C_4H_8O_2$, $(\mathbf{3})_2$, and **4**.

	$2(\mathbf{1})_3 \cdot Et_2O$	$[\mathbf{2} \cdot (C_4H_8O_2)_2] \cdot 3C_4H_8O_2$	$(\mathbf{3})_2$	**4**
Formula	$C_{76}H_{106}Ge_6O_{13}$	$C_{68}H_{104}Ge_4O_{18}$	$C_{48}H_{64}Ge_2O_6$	$C_{19}H_{26}GeN_2O_2$
Molecular mass [g mol^{-1}]	1663.14	1499.87	882.17	387.01
Temperature [K]	110	100	100	110
Wavelength [Å]	0.71073	1.54184	0.71073	0.71073
Crystal system	monoclinic	triclinic	monoclinic	monoclinic
Space group	$P2_1/c$	$P\bar{1}$	$P2_1/n$	$P2_1/n$
Crystal size [mm^3]	0.30 × 0.10 × 0.04	0.12 × 0.04 × 0.02	0.40 × 0.40 × 0.20	0.40 × 0.30 × 0.30
a [Å]	15.0464(3)	9.0781(10)	15.1462(5)	8.8986(4)
b [Å]	11.3329(3)	13.2094(13)	7.0767(2)	20.5100(9)
c [Å]	23.1488(5)	15.2661(15)	21.7259(7)	10.5958(5)
α [°]		100.391(8)		
β [°]	103.963(2)	95.373(8)	107.190(4)	94.277(4)
γ [°]		98.029(9)		
V [Å^3]	3830.68(15)	1769.7(3)	2224.67(12)	1928.46(15)
Z	2	1	2	4
Density, calcd. [Mg m^{-3}]	1.442	1.407	1.317	1.333
μ [mm^{-1}]	2.382	2.510	1.398	1.601
F (000)	1716	784	928	808
θ range for data collection [°]	2.938–25.00	4.08–62.08	2.92–25.25	3.036–24.993
Index ranges	$-17 \le h \le 15$ $-9 \le k \le 13$ $-27 \le l \le 27$	$-10 \le h \le 8$ $-12 \le k \le 15$ $-17 \le l \le 15$	$-12 \le h \le 18$ $-8 \le k \le 8$ $-25 \le l \le 26$	$-9 \le h \le 10$ $-15 \le k \le 24$ $-11 \le l \le 12$
Reflections collected	15872	9835	10811	7800
Independent reflections	6710 [R(int.) = 0.0309]	5466 [R(int.) = 0.0786]	4012 [R(int.) = 0.0332]	3383 [R(int.) = 0.0228]
Data	6710	5466	4012	3383
Goodness-of-fit on F^2	1.036	0.933	1.059	1.041
Final R indices [$I > 2\sigma(I)$], $\omega R_2(F^2)$ (all data)	$R1$ = 0.0349, wR_2 = 0.0884	$R1$ = 0.0998, wR_2 = 0.2618	$R1$ = 0.0341, wR_2 = 0.0883	$R1$ = 0.0302, wR_2 = 0.0721
Largest diff. peak and hole [e Å^{-3}]	0.890 and –0.607	2.434 and –1.041	0.423 and –0.580	0.373 and –0.369

supplementary crystallographic data for this paper. These data can be obtained free of charge from The Cambridge Crystallographic Data Centre via www.ccdc.cam.ac.uk/data_request/cif.

Computational Details: The quantum chemical calculations of energies were carried out at the DFT-D (B3LYP-D3/def2-TZVPP) level of theory using the TURBOMOLE program package.[29] All structure data given as *xyz*-files in the Supporting Material were obtained by relaxing all degrees of freedom. The optimized structures of the species $(\mathbf{1})_5$ and $(\mathbf{C})_5$ were estimated to be energetically favorable structures. All other structures were confirmed as minima by normal mode analysis.

Acknowledgments

We gratefully acknowledge financial support by the Deutsche Forschungsgemeinschaft (DFG) (Forschergruppe 1497, Organic-Inorganic Nanocomposites through Twin Polymerization) and the Fonds der Chemischen Industrie for Ph. D. fellowships to P. K. and M. K. We also thank Dr. H. Petzold for NMR spectroscopic measurements at variable temperatures.

[1] D. H. Harris, M. F. Lappert, *J. Chem. Soc., Chem. Commun.* **1974**, 895–896.
[2] a) H. Sakaba, Y. Arai, K. Suganuma, E. Kwon, *Organometallics* **2013**, *32*, 5038–5046; b) I. A. Portnyagin, M. S. Nechaev, *J. Organomet. Chem.* **2009**, *694*, 3149–3153; c) J. Hlina, J. Baumgartner, C. Marschner, P. Zark, T. Müller, *Organometallics* **2013**, *32*, 3300–3308; d) N. Zhao, J. Zhang, Y. Yang, G. Chen, H. Zhu, H. W. Roesky, *Organometallics* **2013**, *32*, 762–769; e) D. Matioszek, N. Saffon, J.-M. Sotiropoulos, K. Miqueu, A. Castel, J. Escudie, *Inorg. Chem.* **2012**, *51*, 11716–11721; f) L. W. Pineda, V. Jancik, J. F. Colunga-Valladares, H. W. Roesky, A. Hofmeister, J. Magull, *Organometallics* **2006**, *25*, 2381–2383.
[3] a) L. Wang, S.-C. Rosca, V. Poirier, S. Sinbandhit, V. Dorcet, T. Roisnel, J.-F. Carpentier, Y. Sarazin, *Dalton Trans.* **2014**, *43*, 4268–4286; b) D. Gallego, A. Brück, E. Irran, F. Meier, M. Kaupp, M. Driess, J. F. Hartwig, *J. Am. Chem. Soc.* **2013**, *135*, 15617–15626; c) K. Revunova, G. I. Nikonov, *Dalton Trans.* **2015**, *44*, 840–866.
[4] a) Z. D. Brown, P. P. Power, *Inorg. Chem.* **2013**, *52*, 6248–6259; b) Z. D. Brown, P. Vasko, J. D. Erickson, J. C. Fettinger, H. M. Tuononen, P. P. Power, *J. Am. Chem. Soc.* **2013**, *135*, 6257–6261; c) J. W. Dube, Z. D. Brown, C. A. Caputo, P. P. Power, P. J. Ragogna, *Chem. Commun.* **2014**, *50*, 1944–1946; d) Z. D. Brown, J. D. Erickson, J. C. Fettinger, P. P. Power, *Organometallics* **2013**, *32*, 617–622.
[5] a) A. V. Zabula, F. E. Hahn, *Eur. J. Inorg. Chem.* **2008**, 5165–5179; b) O. Kühl, *Coord. Chem. Rev.* **2004**, *248*, 411–427; c) S. Karwasara, M. K. Sharma, R. Tripathi, S. Nagendran, *Organometallics* **2013**, *32*, 3830–3836; d) S. Krupski, R. Poettgen, I. Schellenberg, F. E. Hahn, *Dalton Trans.* **2014**, *43*, 173–181.
[6] a) R. A. Green, C. Moore, A. L. Rheingold, C. S. Weinert, *Inorg. Chem.* **2009**, *48*, 7510–7512; b) C. S. Weinert, A. E. Fenwick, P. E. Fanwick, I. P. Rothwell, *Dalton Trans.* **2003**, 532–539; c) T. J. Boyle, L. J. Tribby, L. A. M. Ottley, S. M. Han, *Eur. J. Inorg. Chem.* **2009**, 5550–5560; d) B. Cetinkaya, I. Gumrukcu, M. F. Lappert, J. L. Atwood, R. D. Rogers, M. J. Zaworotko, *J. Am. Chem. Soc.* **1980**, *102*, 2088–2089; e) M. F. Lappert, R. S. Rowe, *Coord. Chem. Rev.* **1990**, *100*, 267–292; f) A. J. Ruddy, P. A. Rupar, K. J. Bladek, C. J. Allan, J. C. Avery, K. M. Baines, *Organometallics* **2010**, *29*, 1362–1367.
[7] a) M. Huang, M. M. Kireenko, P. B. Djevakov, K. V. Zaitsev, Y. F. Oprunenko, A. V. Churakov, D. A. Tyurin, S. S. Karlov, G. S. Zaitseva, *J. Organomet. Chem.* **2013**, *735*, 15–25; b) M. Huang, M. M. Kireenko, K. V. Zaitsev, Y. F. Oprunenko, A. V. Churakov, J. A. K. Howard, E. K. Lermontova, D. Sorokin, T. Linder, J. Sundermeyer, S. S. Karlov, G. S. Zaitseva, *Eur. J. Inorg. Chem.* **2012**, 3712–3724; c) M. Huang, E. K. Lermontova, K. V. Zaitsev, A. V. Churakov, Y. F. Oprunenko, J. A. K. Howard, S. S. Karlov, G. S. Zaitseva, *J. Organomet. Chem.* **2009**, *694*, 3828–3832; d) T. Heidemann, S. Mathur, *Eur. J. Inorg. Chem.* **2014**, 506–510.
[8] A. E. Wetherby Jr., L. R. Göller, A. G. DiPasquale, A. L. Rheingold, C. S. Weinert, *Inorg. Chem.* **2008**, *47*, 2162–2170.
[9] a) A. E. Wetherby Jr., L. R. Göller, A. G. DiPasquale, A. L. Rheingold, C. S. Weinert, *Inorg. Chem.* **2007**, *46*, 7579–7586; b) T. Hascall, K. Pang, G. Parkin, *Tetrahedron* **2007**, *63*, 10826–10833; c) T. Hascall, G. Parkin, A. L. Rheingold, I. Guzei, *Chem. Commun.* **1998**, 101–102; d) B. G. McBurnett, A. H. Cowley, *Chem. Commun.* **1999**, 17–18.
[10] Y. Peng, J.-D. Guo, B. D. Ellis, Z. Zhu, J. C. Fettinger, S. Nagase, P. P. Power, *J. Am. Chem. Soc.* **2009**, *131*, 16272–16282.
[11] a) K. A. Miller, T. W. Watson, J. E. Bender, M. M. B. Holl, J. W. Kampf, *J. Am. Chem. Soc.* **2001**, *123*, 982–983; b) W. P. Neumann, *Chem. Rev.* **1991**, *91*, 311–334; c) P. Jutzi, H. Schmidt, B. Neumann, H. G. Stammler, *Organometallics* **1996**, *15*, 741–746.
[12] H. Ohgaki, W. Ando, *J. Organomet. Chem.* **1996**, *521*, 387–389.
[13] P. Riviere, J. Satgé, A. Boy, *J. Organomet. Chem.* **1975**, *96*, 25–40.
[14] a) M. Huang, M. M. Kireenko, K. V. Zaitsev, Y. F. Oprunenko, A. V. Churakov, J. A. K. Howard, M. V. Zabalov, E. K. Lermontova, J. Sundermeyer, T. Linder, S. S. Karlov, G. S. Zaitseva, *J. Organomet. Chem.* **2012**, *706*, 66–83; b) A. E. Wetherby Jr., C. R. Samanamu, A. C. Schrick, A. DiPasquale, J. A. Golen, A. L. Rheingold, C. S. Weinert, *Inorg. Chim. Acta* **2010**, *364*, 89–95; c) E. Bonnefille, S. Mazieres, N. El Hawi, H. Gornitzka, C. Couret, *J. Organomet. Chem.* **2006**, *691*, 5619–5625; d) K. A. Miller, J. M. Bartolin, R. M. O'Neill, R. D. Sweeder, T. M. Owens, J. W. Kampf, M. M. B. Holl, N. J. Wells, *J. Am. Chem. Soc.* **2003**, *125*, 8986–8987.
[15] J. L. Walding, P. E. Fanwick, C. S. Weinert, *Inorg. Chim. Acta* **2005**, *358*, 1186–1192.
[16] J. K. West, L. Stahl, *Organometallics* **2012**, *31*, 2042–2052.
[17] L. Lange, B. Meyer, W. W. Dumont, *J. Organomet. Chem.* **1987**, *329*, C17–C20.
[18] a) L. Roß, M. Dräger, *Z. Naturforsch. B* **1984**, *39*, 868–875; b) M. Nanjo, T. Sasage, K. Mochida, *Chem. Lett.* **2002**, 1124–1125; c) M. Nanjo, T. Sasage, K. Mochida, *J. Organomet. Chem.* **2003**, *667*, 135–142; d) M. P. Brown, E. G. Rochow, *J. Am. Chem. Soc.* **1960**, *82*, 4166–4168; e) K. Ogawa, K. Tanaka, S. Yoshimura, Y. Takeuchi, J. Chien, Y. Kai, N. Kasai, *Acta Crystallogr., Sect. C: Cryst. Struct. Commun.* **1991**, *47*, 2558–2561.
[19] a) H. Puff, S. Franken, W. Schuh, W. Schwab, *J. Organomet. Chem.* **1983**, *254*, 33–41; b) H. Puff, S. Franken, W. Schuh, W. Schwab, *J. Organomet. Chem.* **1983**, *244*, C41–C42.
[20] J. Beckmann, K. Jurkschat, M. Schürmann, *Eur. J. Inorg. Chem.* **2000**, 939–941.
[21] P. Klüfers, C. Vogler, *Z. Anorg. Allg. Chem.* **2007**, *633*, 908–912.
[22] M. Mantina, A. C. Chamberlin, R. Valero, C. J. Cramer, D. G. Truhlar, *J. Phys. Chem. A* **2009**, *113*, 5806–5812.
[23] a) A. K. Swarnakar, S. M. McDonald, K. C. Deutsch, P. Choi, M. J. Ferguson, R. McDonald, E. Rivard, *Inorg. Chem.* **2014**, *53*, 8662–8671; b) B. Lyhs, D. Bläser, C. Wölper, S. Schulz, R. Haack, G. Jansen, *Inorg. Chem.* **2013**, *52*, 7236–7241; c) A. Jana, V. Huch, D. Scheschkewitz, *Angew. Chem. Int. Ed.* **2013**, *52*, 12179–12182.
[24] V. Krishnan, S. Gross, S. Müller, L. Armelao, E. Tondello, H. Bertagnolli, *J. Phys. Chem. B* **2007**, *111*, 7519–7528.
[25] C.-L. Lin, M.-D. Su, S.-Y. Chu, *Chem. Phys.* **1999**, *249*, 145–160.
[26] P. Kitschke, A. A. Auer, T. Löschner, A. Seifert, S. Spange, T. Rüffer, H. Lang, M. Mehring, *ChemPlusChem* **2014**, *79*, 1009–1023.

[27] T. Fjeldberg, A. Haaland, B. E. R. Schilling, M. F. Lappert, A. J. Thorne, *J. Chem. Soc., Dalton Trans.* **1986**, 1551–1556.
[28] G. M. Sheldrick, *Acta Crystallogr., Sect. A* **2008**, *64*, 112–122.
[29] a) A. D. Becke, *J. Chem. Phys.* **1993**, *98*, 5648–5652; b) C. Lee, W. Yang, R. G. Parr, *Phys. Rev. B* **1988**, *37*, 785–789; c) R. Ahlrichs, M. Bär, M. Häser, H. Horn, C. Kölmel, *Chem. Phys. Lett.* **1989**, *162*, 165–169; d) R. Ahlrichs, O. Treutler, *J. Chem. Phys.* **1995**, *102*, 346–354; e) M. v. Arnim, R. Ahlrichs, *J. Comput. Chem.* **1998**, *19*, 1746–1757; f) F. Weigend, M. Häser, H. Patzelt, R. Ahlrichs, *Chem. Phys. Lett.* **1998**, *294*, 143–152; g) F. Weigend, R. Ahlrichs, *Phys. Chem. Chem. Phys.* **2005**, *7*, 3297–3305; h) S. Grimme, J. Antony, S. Ehrlich, H. Krieg, *J. Chem. Phys.* **2010**, *132*, 154104.

Received: September 29, 2015
Published Online: October 28, 2015

